Structural Engineering and Mechanics, Vol. 4, No. 5 (1996) 485-496
DOI: http://dx.doi.org/10.12989/sem.1996.4.5.485

Stability and failure of symmetrically laminated plates

Gin Boay Chai† and Kay Hiang Hoon†

Division of Engineering Mechanics, School of Mechanical and Production Engineering, Nanyang Technological University, Nanyang Ave., 2263 Singapore

Sin Sheng Chin‡

Materials Research Division, Defence Science Organization, Ministry of Defence, Singapore

Ai Kah Soh‡†

GINTIC Institute of Manufacturing Technology, Nanyang Ave., Singapore

Abstract. This paper describes a numerical and experimental study on the stability and failure behaviour of rectangular symmetric laminated composite plates. The plates are simply supported along the unloaded edges and clamped along the loaded ends, and they are subjected to uniaxial in-plane compression. The finite element method was employed for the theoretical study. The study examines the effect of the plate's stacking sequence and aspect ratio on the stability and failure response of rectangular symmetric laminated carbon fibre reinforced plastics composite plates. The study also includes the effect of the unloaded edge support conditions on the postbuckling response and failure of the plates. Extensive experimental investigation were also carried out to supplement the finite element study. A comprehensive comparison between theory and experimental data are presented and discussed in this contribution.

Key words: stability; laminated composites; postbuckling; failure; flat panels.

1. Introduction

The increasing use of composite materials has led to the significance of the study of structural analysis of composite. Composites are known for their high strength to weight ratio as well as high specific stiffness. Other properties of composites include resistance to fatigue, corrosion and design flexibility. The main demand is contributed by the aircraft and aerospace industries where the materials are employed mainly in aircraft fuselage, wings, doors and control surfaces while the bulk of aircraft structures are made of metallic materials. For lightly loaded region such as the metallic fuselage, in particular, the post-buckling strength up to proof or ultimate failure is utilised. In order to complete using composite material, the same design criteria for metals has to be applied.

† Senior Lecturer
‡ Project Engineer
‡† Group Manager

A literature search of related technical publications has shown that most of the research were biased towards theoretical analyses of composite structures and there seems to be a lack of experimental investigative publications. Due to these factors, designers are reluctant to use the post-buckling strength beyond the initial buckling load in their criteria. It is well known that the postbuckling strength of composite panel can reach as high as two to five times the buckling load as documented in Banks and Harvey (1978), Buskell, Davies and Stevens (1985), Chai, Banks and Rhodes (1989), Natsiava, Babcock and Knauss (1990) and Chai, Banks and Rhodes (1991). This means that a considerable amount of post-buckling strength can be exploited.

Several technical papers have been published on the buckling and postbuckling of composite panels. Leissa (1981, 1987) and Kapania and Raciti (1989) in a recent contribution have found vast and varied ranges of literatures related to this field of research. Failure of composite plates in compression was postulated to be initiated from the free edge at the buckle node as reported by Starnes and Rouse (1981), Ridgard (1983) and Davies, Buskell and Stevens (1986). The main cause is the high interlaminar shear stresses leading to the initiation of delamination failure. Research publication in this area is however limited and a failure criterion to identify postbuckling failure is urgently required. The present study uses the finite element method coupled with the well known Tsai-Wu failure criterion to predict postbuckling failure in laminated composite plates. In addition an extensive expreimental programme was carried out to complement the theoretical study. The results of the numerical and experimental investigations carried out in this study will help to enhance the present understanding of the stability and failure behaviour of laminated composite panels subjected to in-plane compression.

2. Numerical procedures

The test panels were modelled using a commercially available finite element software computer source code (ANSYS 1989) for the numerical study of the buckling, post-buckling and failure behaviour. The element type used was the 8 noded isoparametric layered shell element with 6 degrees of freedom at each node. The formulation of this shell element is based on the three

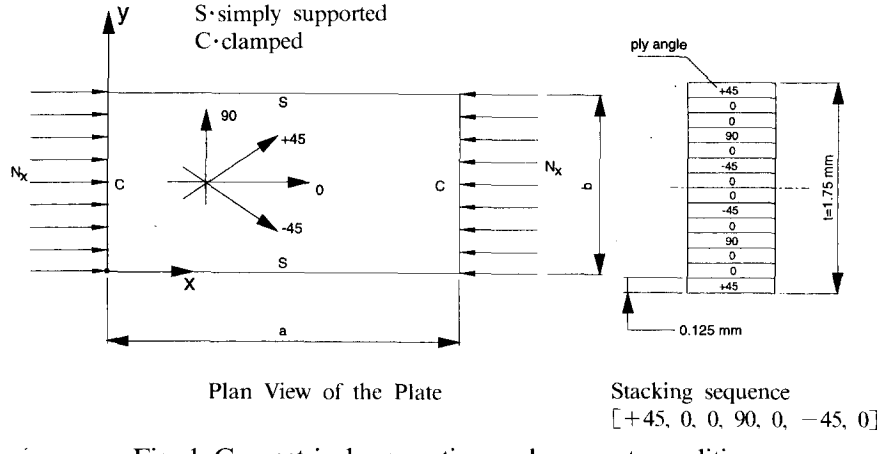

Fig. 1 Geometrical properties and support conditions.

Table 1 Description of test plate specimens

Test specimens	Aspect ratio, a/b	Laminate thickness, t (mm)	Stacking sequence
76A1,76A2	458/76	1.75	Type A
76B1,76B2	458/76	1.75	Type B
76C1,76C2	458/76	1.75	Type C
90A1,90A2	458/90	1.75	Type A
90B1,90B2	458/90	1.75	Type B
90C1,90C2	458/90	1.75	Type C
114A1,114A2	458/114	1.75	Type A
114B1,114B2	458/114	1.75	Type B
114C1,114C2	458/114	1.75	Type C

Type A: [+45/0/0/90/0/-45/0]s
Type B: [+45/0/0/90/0/0/-45]s
Type C: [0/0/90/0/0/+45/-45]s

dimensional elasticity approach of Ahmad, Irons and Zienkiewicz (1970). The boundary conditions prescribed on the model are shown in Fig. 1. The material properties of the unidirectional Grafil XAS/914C layer used in the analysis are: $E_{11}=130$ GPa, $E_{22}=9$ GPa, $G_{12}=4.8$ GPa, $\nu_{12}=0.28$, Longitudinal tensile strength, $X_t=1.4$ GPa, Transverse tensile strength, $Y_t=0.79$ GPa, Longitudinal compressive strength, $X_c=1.35$ GPa, Transverse compressive strength, $Y_c=0.23$ GPa and Interlaminar shear strength, $S=0.078$ GPa.

2.1. Buckling analysis

In the preliminary numerical study, a panel of dimension 90 mm×458 mm×1.75 mm with Type *A* stacking sequence was modelled for buckling analysis. Details of the geometry and stacking sequence of the test panels are described in Table 1. The buckling analysis was performed using the full subspace eigenvalue extraction procedures as described in Bathe (1982). The converged buckling load of 9.064 kN was obtained using a mesh size of 64 elements for this plate, the convergence tolerance being 1.0*e*-6. Similarly converged buckling results are obtained for test plates with width of 76 mm and 114 mm and of different stacking sequence of which details will be discussed later when comparing with experimental data. The buckled modal shapes obtained in this analysis will be used as the initial imperfections of the plates in the post-buckling analysis later on.

2.2. Post-buckling analysis

To perform a non-linear analysis, some form of out-of-plane perturbation such as a modest temporary force or specified deflection must be imposed on the model to initiate the buckling response. For the case of thin plate in compression, Yusuff (1952), Coan (1959) and Yamaki (1959) showed that initial geometrical imperfection should be of the same form as the buckled modal shape. Thus the number of half sine waves prescribed as initial imperfection in the plate for the post-buckling analysis is based on the buckled shape obtained from the buckling analysis. The usual sine function is used for the initially prescribed imperfection:

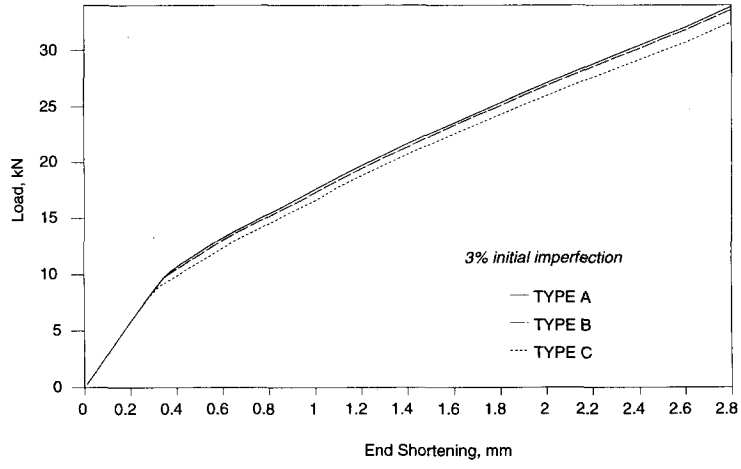

Fig. 2 Graph of load *vs* end shortening.

$$W_0 = A_0 \sin\left(\frac{m\pi x}{a}\right)\sin\left(\frac{\pi y}{b}\right) \tag{1}$$

where A_0 is the amplitude of sine wave, a is the length of the plate, b is the width of the plate and m is the number of half sine waves. A four half sine waves ($m=4$) initial imperfection was prescribed in test plates with aspect ratio 458/90. An initial prescribed imperfection form of three and five half sine waves were chosen for test plates with aspect ratio 458/114 and 458/76 respectively. The degree of initial imperfection represents the maximum amplitude of the imperfection curve as a percentage of the plate thickness. It was observed that during the analysis phase the incremental step-size of the applied end shortening and the degree of prescribed initial imperfection affect the bifurcation region, details of this investigation can be found in Chai and Hoon (1994).

An initial imperfection of 3% was used for the plate models in study. The mesh size of 245 elements, 324 elements and 294 elements were selected for test plates with aspect ratios 458/90, 458/114 and 458/76 respectively. Mesh size selections were based on the reasonable converged results with minimum computational time. Fig. 2 shows the finite element results for the three plate models in which the plate's aspect ratio is 458/90 and the stacking sequence varies. It can be seen that the postbuckling stiffnesses are the same for the three different type of stacking sequence and if plotted non-dimensionally the three curves will unified. This observation is also true for plate's aspect ratio of 458/76 and 458/114.

2.3. Failure analysis

The failures of the finite element plate model was investigated with the Tsai-Wu failure criteria, Tsai and Wu (1971). The Tsai-Wu criteria used here is the three-dimensional version reported in Tsai and Wu (1971) and it is described by:

$$\zeta = \left(\frac{1}{X_t}+\frac{1}{X_c}\right)\sigma_x + \left(\frac{1}{Y_t}+\frac{1}{Y_c}\right)\sigma_y + \left(\frac{1}{Z_t}+\frac{1}{Z_c}\right)\sigma_z - \frac{\sigma_x^2}{X_t X_c} - \frac{\sigma_y^2}{Y_t Y_c} - \frac{\sigma_z^2}{Z_t Z_c}$$

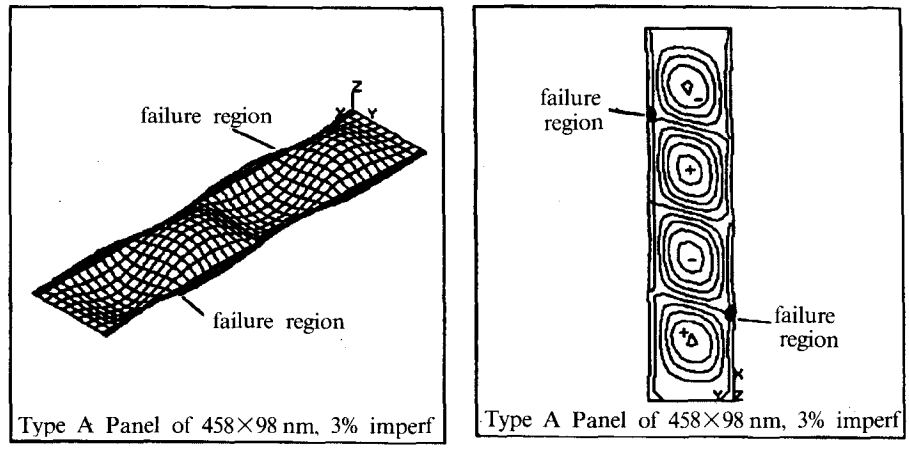

(a) Isometric view of a typically deformed plate (b) Plan contour view of a typically deformed plate

Fig. 3 Predicted regions of failure.

$$+\left(\frac{\sigma_{xy}}{S_{xy}}\right)^2+\left(\frac{\sigma_{yz}}{S_{yz}}\right)^2+\left(\frac{\sigma_{xz}}{S_{xz}}\right)^2+\frac{C_{xy}\sigma_x\sigma_y}{\sqrt{X_tX_cY_tY_c}}+\frac{C_{yz}\sigma_y\sigma_z}{\sqrt{Y_tY_cZ_tZ_c}}+\frac{C_{xz}\sigma_x\sigma_z}{\sqrt{X_tX_cZ_tZ_c}} \tag{2}$$

where X_t is the tensile strength in the x-direction, X_c is the compressive strength in the x-direction, Y_t is the tensile strength in the y-direction, Y_c is the compressive strength in the y-direction, Z_t is the tensile strength in the z-direction, Z_c is the compressive strength in the z-direction, S_{xy} is the shear strength in the xy-plane, S_{yz} is the shear strength in the yz-plane, S_{xz} is the shear strength in the xz-plane, C_{xy} is the x-y coupling coefficient, C_{yz} is the y-z coupling coefficient and C_{xz} is the x-z coupling coefficient.

In the above equation, properties in the z-direction are taken as identical to properties in the y-direction. The coupling coefficients used in the computation are those recommended by Tsai and Wu (1971) and failure in the finite element model occurs when the parameter ζ is equal to or greater than one. A typical failure description of a plate model using the finite element method is plotted in Fig. 3. The figure shows the predicted areas of the first ply failure in a Type A plate of aspect ratio 458/90. Through the thickness, failure was predicted to initiate at the-45° layer.

3. Experimental set-up

Fig. 4 shows an illustration of the experimental set up. The loading machine, Instron 4205, provide the loading at uniform displacement step on the test rig. The TV laser holographic sensor unit (Retra system) containing the laser, lens arrangement and the camera was placed in front of the test specimen at coherent length of 1040 mm. The coherent length was minimum distance for total destructive or constructive fringes to be seen on monitor, the former being dark fringe while the latter bright fringe. The coherent length could be reduced to 740 mm such as to allow a magnified view. A retroreflective tape was pasted over the dull composite surfaces of each test plate such that most of the expanded laser beam shone on the surface were reflected

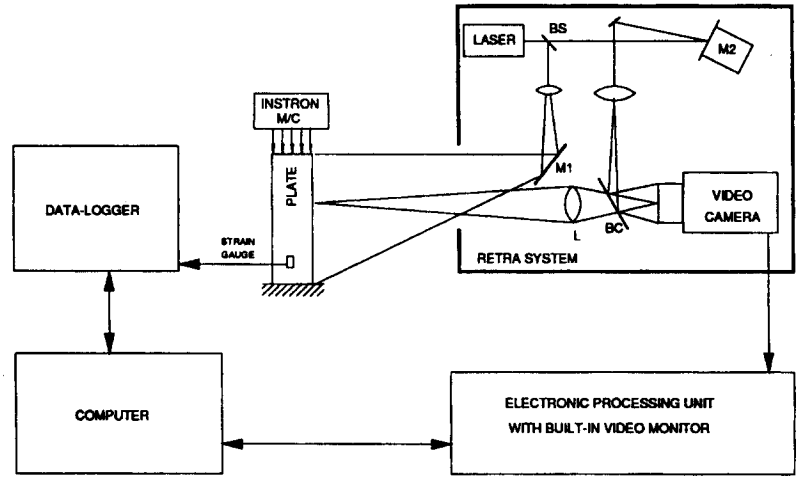

Fig. 4 Schematic drawing of the test set-up.

towards the camera to give a more contrasted interferometric pattern.

3.1. Testing procedures

The test plates were made with 14 layers of Grafil XAS unidirectional carbon fibers preimpregnated in 914C Fibredux epoxy resin. The dimensions of these plates are summarised in Table 1, where a is the length, b is the width and t is the total laminate thickness of the plate. Prior to testing, the test plate was clamped on the short sides by a top and a bottom platen and the simple supports on the long sides were simulated by knife edges. Each plate overhung the knife edges by 6.5 mm, this allows the edges to wave-in during the post-buckling and thus to prevent premature failure. These knife edges were also coated with grease to reduce frictional effect and thus ensured the sides of the plate were free to wave in-plane and remained stress free. The assembled test rig was then placed on the loading machine. The test plate was also subjected to a sequence of loading and unloading to allow the plate to settle into the test rig and take up any movement between the components of test rig. This was carried everytime prior to actual testing and recording of data.

During the test, the load was increased at a uniform displacement rate of 0.05 mm/min. At certain load levels, the strain gauges readings were recorded. The holographic images of the deformed plate at incremental load steps are continuously recorded by video recorder via a camera. And these are relayed to the electronic processing unit and frame grabbing device to enable the holographic image to be captured on the monitor. The automatic frame grabbing facility allows the reference frame to be captured every half a second, hence the model shape at buckling can be recorded in-situ. The personal computer stores the necessary image processing hardware and software to enhance the image captured.

4. Discussions

The problem associated with the determination of the experimental buckling load in isotropic

Table 2 Comparison of buckling load ratios

Test plate	#*Pe/Pn*	**Pe/Pn*	@*Pe/Pn*
76A1	1.25	1.09	1.07
76A2	1.02	1.03	–
76B1	1.11	1.02	1.18
76B2	1.12	1.12	1.04
76C1	1.67	1.13	1.16
76C2	1.35	1.07	1.19
90A1	1.2	1.10	1.18
90A2	1.25	1.11	1.08
90B1	1.45	1.10	–
90B2	1.54	1.09	1.10
90C1	1.06	1.27	–
90C2	1.34	1.19	1.20
114A1	1.21	1.07	0.97
114A2	1.19	1.04	1.04
114B1	1.21	1.15	1.22
114B2	1.06	1.04	1.11
114C1	1.23	1.04	1.14
114C2	1.14	1.04	1.14

Pe obtained from the knee of the load *vs* end shortening curve
* *Pe* obtained from intersection of the membrane strain curve
@ *Pe* obtained using TV-laser holography
Pn is the predicted buckling load

plates accurately has been well research by numerous workers including Coan (1959) and Yamaki (1959). These problems equally apply to composite plates as shown by Chai (1991). Two methods for obtaining the experimental buckling load were commonly used-the first method estimates the buckling load from the "knee" of the load versus end shortening curve while the second method estimates the buckling load from the intersection of the tangents of the prebuckling curve to the postbuckling curve of the load versus membrane strain curves. The second method is more popular and has been shown in the past to give a reasonable buckling load prediction. The results obtained using TV-laser holography will also be presented here for comparison. The buckling load obtained using TV-laser holography is taken at the instant the buckle mode shape appeared on the TV monitor. This method using the TV-laser holography for the determination of the buckling load has not been reported before as far as the authors know.

The results for the 14 plates tested are tabulated in Table 2 as ratio of the experimental buckling load over the predicted buckling load. It is obvious that the second method for obtaining the buckling load experimentally correlates better with the predicted results. Table 2 also shows the experimental results obtained using TV-laser holography method. It can be seen that their results on the whole, considering that their results can be obtained in-situ, are as good as the results obtained using the second method.

Figs. 5, 6 and 7 compare the predicted load versus end shortening behaviour with the corresponding experimental data for test plates with aspect ratio 458/76, 458/90 and 458/114 respectively. Two theoretical curves are presented in these graphs, one for the case where the unloaded edges are clamped and the other for the case when the unloaded edges are simply-supported. The

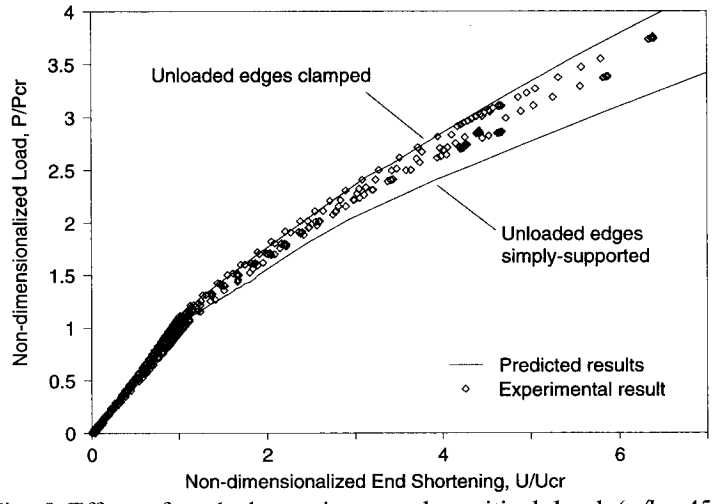

Fig. 5 Effect of end shortening on the critical load (a/b=458/76).

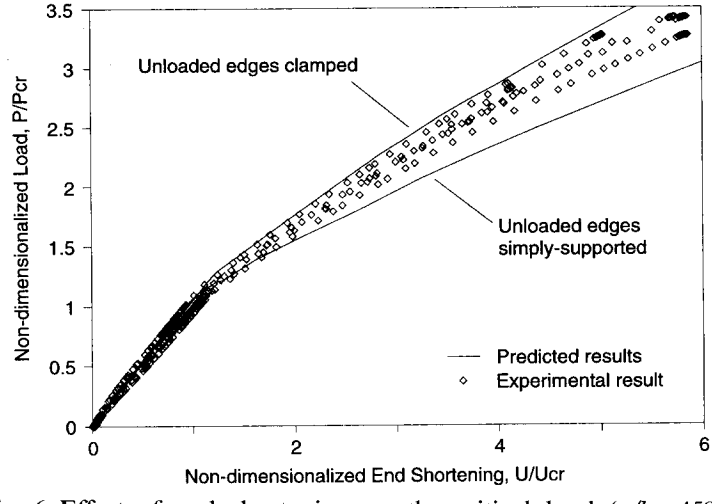

Fig. 6 Effect of end shortening on the critical load (a/b=458/90).

figures suggested that these two curves represent the upper and lower bound solution to the present test data. The comparison also shows that the actual simulation of simple support conditions along the knife edges of the test plate is not achieved. This is probably the main reason that the experimental buckling loads are always higher than the predicted ones which are based on simply supported unloaded edges. Therefore it can be concluded that some degree of edge restraints were present during the testing process and this also explains the higher experimental buckling loads of the test plates in Table 2.

The experimentally obtained failure loads of the test plates are tabulated in Table 3 together with the corresponding predicted failure loads. It can be seen from the table that the numerical prediction of failure load using the Tsai-Wu failure criterion gives a lower and thus conservative value for all the test plates. However one must bear in mind that experimentally measured

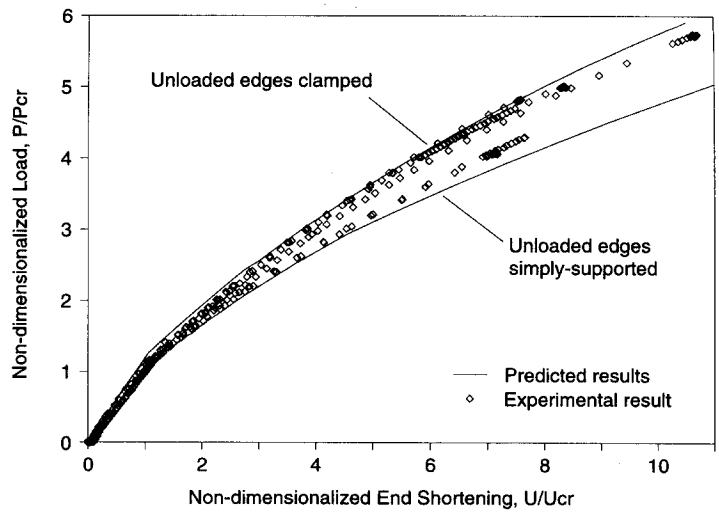

Fig. 7 Effects of end shortening on the critical load (a/b=458/114).

Table 3 Comparing experimentally obtained failure load with predicted results

Test plates	Predicted failure (kN)	Measured failure (kN)	Predicted P_f/P_{cr}	Measured P_f/P_{cr}
76A1	23.00	28.64	2.18	2.48
76A2	23.00	28.79	2.18	2.66
76B1	22.35	29.20	2.18	2.70
76B2	22.35	30.42	2.18	2.65
76C1	25.25	37.50	2.84	3.74
76C2	25.25	*34.95	2.84	3.65
90A1	22.41	31.20	2.48	3.41
90A2	22.41	*31.23	2.48	*3.10
90B1	22.50	32.80	2.56	3.38
90B2	22.50	32.76	2.56	3.42
90C1	26.80	*32.90	3.56	*3.42
90C2	26.80	*26.99	3.56	*3.01
114A1	22.55	32.11	3.06	4.07
114A2	22.55	31.71	3.06	4.16
114B1	25.63	29.11	3.58	3.55
114B2	25.63	34.59	3.58	4.62
114C1	28.22	38.60	4.35	5.70
114C2	28.22	33.84	4.35	5.00

P_f experimental ultimate failure load
P_{cr} buckling load
* not tested to ultimate failure loading

failures are ultimate while theoretically obtained failures are indications of initial failures. In other words if the theoretical analysis had included the multiple plies failure procedures then the ultimate failure load will no doubt be higher than the load to cause first-ply failure.

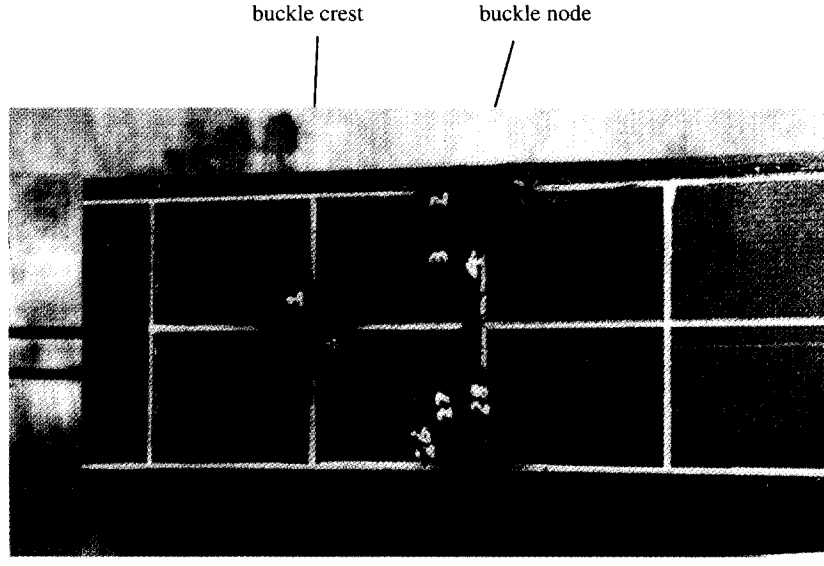

Fig. 8 Photograph of actual failure at the edge.

In all the plates tested, some of the failures were observed to have occurred at the edge of the buckle nodal line, see Fig. 8, as predicted by the finite element analysis. Unfortunately some test plates failed prematurely due to the design features of the test rig. These failures occurred near the top clamped ends of the specimen, in the region where a 5 mm gap was allowed at the top platen of rig for the end compression. Nevertheless in many of these prematurely failed specimens, cracks were observed to have initiated near the free edge of the buckle nodal line which would have caused final failure.

5. Concluding remarks

A linear buckling and a non-linear postbuckling analysis was carried out using the finite element method. The finite element results based on a plate model with unloaded edges simply-supported predicted the buckling load to within a 20% deviation from the test data and predicted the failure loads of the laminated composite plates to within 33% deviation from the test data obtained. The possible reasons for these deviations were also mentioned and discussed in the paper. It was shown that the postbuckling behaviour of the test plates tends to correlate better with the theoretical results based on the unloaded edges that are clamped. It was also shown that for a specific plate dimension, plate with Type *A* stacking sequence tend to give a highest buckling load but the lowest failure load, whereas plate with Type *C* stacking sequence gives the lowest buckling but the highest failure load. It was also observed that extreme care must be taken during the setting up of the test rig such that the knife edges really stimulate simple support conditions.

Acknowledgements

The authors would like to extend their appreciation to the Ministry of Finance. Singapore for funding this project under the grant MOF R & D 5/89 and to British Aerospace plc. U.K. for supplying the test plates. The authors are also grateful to the undergraduate students involved in both the theoretical and experimental programmes.

References

Ahmad, S., Irons, B.M. and Zienkiewicz, O.C. (1970), "Analysis of thick and thin shell structures by curved finite elements", *International Journal for Numerical Methods in Engineering,* **2**(3), 419-451.

ANSYS (1989), *Engineering Analysis System Theoretical Manual,* Revision 4.4, edited by Peter C. Kohnke, Swanson Analysis System Inc., Pennsylvannia, U.S.A.

Banks, W.M. and Harvey, J.M. (1978), "Experimental study of stability problems in composite materials", *Stability Problems in Engineering Structures and Components,* edited by T.H. Richards and P. Stanley, Applied Science Publishers Ltd, London, 1-22.

Bathe, K.J. (1982), *Finite Element Procedures in Engineering Analysis,* Prentice-Hall, Englewood Cliffs.

Buskell, N., Davies, G.A.O. and Stevens, K.A. (1985), "Postbuckling failure of composite plates", *Proceedings of the Third International Conference on Composite Structures,* 290-314.

Chai, G.B., Banks, W.M. and Rhodes, J. (1989), "Experimental study on the buckling and postbuckling of carbon fibre composite plates with and without interply disbonds", *Proceedings of IMechE Conference on Design in Composite Materials,* Machanical Engineering Publications Ltd, London, 69-85.

Chai, G.B., Banks, W.M. and Rhodes, J. (1991), "An experimental study on laminated plates in compression", *Composite Structures,* **19**, 67-87.

Chai, G.B. and Hoon, K.H. (1994), "Numerical and experimental study of large deflection of symmetrically laminated composite plates in compression", *Structural Engineering and Mechanics,* **2**(4), 359-367.

Chai, G.B. (1991), "Large deflections of laminated composite plates", *Composites Science and Technology,* **42**(4), 349-360.

Coan, J.M. (1959), "Large deflection theory for plates with small initial curvature loaded in edge compression", *Jnl. Appl. Mech.,* **27**, 143.

Davies, G.A.O., Buskell, N. and Stevens, K.A. (1986), "Edge effects in failure of compression plates", *Proceedings of the European Mechanics Colloqium 214, Mechanical Behaviour of Composites and Laminates,* edited by W.A. Green and M. Micunovic, Elsevier Applied Science, Essex, England, 1-11.

Kapania, R.K. and Raciti, S. (1989), "Recent advances in analysis of laminated beams and plates, Part 1: Shear effects and buckling", *AIAA Journal,* **27**(7), 923-934.

Leissa, A.W. (1987), "An overview of composite plate buckling", *Proceedings of the Fourth International Conference on Composite Structures,* **1**, 1-29.

Leissa, A.W. (1981), "Advances in vibration, buckling and postbuckling studies on composite plates", *Composites Structures,* London, Applied Science Publishers Ltd, 312-322.

Natsiavas, S., Babcock, C.D. and Knauss, W.G. (1990), "Postbuckling delamination of a stiffened composite plate using finite elements", *Composite Material Technology,* 1990, edited by D. Hui and T.J. Kozik, *ASME,* New York, 101-106.

Ridgard, C. (1983), "The effects of postbuckling behaviour upon the performance of stability-limited composite structures", *B. Ae-MSM-R-GEN-0509.*

Starnes, J.H. and Rouse, M. (1981), "Postbuckling and failure characteristics of flat rectangular graphite epoxy plates loaded in compression", *Proceedings of AIAA/ASME/ASCE/AHS 22nd Structures, Structural Dynamics and Materials Conference,* Atlanta, Georgia.

Tsai, S.W. and Wu, E.M. (1971), "A general theory of strength for anisotropic materials", *Journal of Composite Materials,* **5**, 58-80.

Yamaki, N. (1959), "Postbuckling behaviour of rectangular plates with small initial curvature loaded

in edge compression", *Jnl. Appl. Mech.*, **26**, 407-414.
Yusuff, S. (1952), "Large deflection theory for orthotropic rectangular plates subjected to edge compression", *Jnl. Appl. Mech.*, **19**, 446-450.